

# Role of Structural Specificity of ZnO Particles in Preserving Functionality of Proteins in their Corona

**Urvashi Singh**

Dayalbagh Educational Institute

**Zeeshan Saifi**

Dayalbagh Educational Institute

**Mridul Kumar**

Dayalbagh Educational Institute

**Armin Reimers**

Kiel University

**Soami Daya Krishnananda** (✉ [ksdaya@dei.ac.in](mailto:ksdaya@dei.ac.in))

Dayalbagh Educational Institute

**Rainer Adelung**

Kiel University

**Martina Baum**

Kiel University

---

## Research Article

**Keywords:** ZnO particles, insulin, MNP-Protein corona

**Posted Date:** July 20th, 2021

**DOI:** <https://doi.org/10.21203/rs.3.rs-364933/v1>

**License:**   This work is licensed under a Creative Commons Attribution 4.0 International License.

[Read Full License](#)

---

**Version of Record:** A version of this preprint was published at Scientific Reports on August 5th, 2021. See the published version at <https://doi.org/10.1038/s41598-021-95540-3>.

# 1 **Role of Structural Specificity of ZnO Particles in Preserving** 2 **Functionality of Proteins in their Corona**

3 **Urvashi<sup>1</sup>, Zeeshan<sup>1</sup>, Mridul Kumar<sup>1</sup>, Armin Reimers<sup>2</sup>, K.S. Daya<sup>1\*</sup>, Rainer Adelung<sup>2</sup>, Martina Baum<sup>2</sup>**

4 <sup>1</sup>Microwave Physics Lab, Department of Physics and Computer Science, Dayalbagh Educational Institute  
5 (Deemed to be University), Dayalbagh, Agra, India

6 <sup>2</sup>Functional Nanomaterial Group, Institute for Material Science, Kiel University, Germany

7 \* Corresponding Author: ksdaya@dei.ac.in

8  
9

10 **ABSTRACT:** Reconfiguration of protein conformation in a micro and nano particle (MNP) protein corona due  
11 to interaction is an often-overlooked aspect in drug design and nano-medicine. Mostly, MNP-Protein corona  
12 studies focus on the toxicity of nano particles (NPs) in a biological environment to analyze biocompatibility.  
13 However, preserving functional specificity of proteins in an NP corona becomes critical for effective translation  
14 of nano-medicine. This paper investigates the non-classical interaction between insulin and ZnO MNPs using a  
15 classical electrical characterization technique at GHz frequency with an objective to understand the effect of the  
16 micro particle (MP) and nanoparticle (NP) morphology on the electrical characteristics of the MNP-Protein  
17 corona and therefore the conformation and functional specificity of protein. The MNP-Protein corona was  
18 subjected to thermal and enzymatic (papain) perturbation to study the denaturation of the protein. Experimental  
19 results demonstrate that the morphology of ZnO particles plays an important role in preserving the electrical  
20 characteristics of insulin.

## 21 **INTRODUCTION:**

22 The size specificity of nanoparticles (NPs) is often considered a primary factor controlling protein adsorption<sup>1-3</sup>.  
23 Additionally, protein adsorption on NPs can also be influenced by their surface morphology, which is  
24 characterized by large surface area and curvature<sup>1-4</sup>. This manuscript primarily aims at examining the roles of  
25 the structural specificity and physicochemical properties of micro and nano particle (MNP) - protein corona in  
26 Nano-Bio interaction.

27 Interactions of protein with other molecules disrupt the electrostatic interaction among the residues which  
28 further leads to conformational changes and in turn affects the protein functions<sup>5,6</sup>. The electrostatic interactions  
29 can also vary by diverse processes such as binding of charged ligands, substitutions of amino acids during site-  
30 directed mutagenesis and also by changes in the tertiary or quaternary structural configurations of the protein  
31 and other bio-molecules<sup>7</sup>. Therefore, electrostatic interaction plays a crucial role in stabilizing protein<sup>7,8</sup>. This  
32 motivates to use electrical parameters of proteins for assessing their structural conformation.

33 Among the several physico-chemical properties<sup>9</sup> which affect the behavior of molecules, the dielectric constant  
34 is an important one. Study of the dielectric properties of proteins is of great interest in the microwave region due  
35 to its spatial variation in orientational polarization leading to temporal change in the dielectric relaxation<sup>10-12</sup>.  
36 The dielectric constant of proteins depends on the distribution of charge residues, side chains and their packing.

37 Tightly and loosely packed regions show low and high dielectric constants respectively<sup>13, 14</sup>. Therefore the  
38 physical state of the bio-macromolecules can be characterized using the dielectric studies which could help to  
39 understand the stability and interaction of protein in a biological media<sup>13, 14</sup>.

40 In-depth protein dynamics like slow and fast spatiotemporal local or collective molecular motions produced by  
41 charge residues can give new understanding about the Nano-Bio interface<sup>15</sup>. To understand the phenomenon  
42 taking place at the molecular level, a theoretical model was developed where it is assumed that the MNP protein  
43 complex suspended in a buffer medium is governed by binding, damping and driving forces, which arise due to  
44 chemical bonding, buffer drag and applied electric field respectively (See Materials and Methods section). By  
45 solving the governing differential equations, a theoretical expression for the mechanical vibration frequency was  
46 derived, which is a function of the dielectric constant and the dipole moment (See Materials and Methods  
47 section). Using microwave resonant technique (See Methods and Supplementary Section), we have studied the  
48 protein along with MNPs under various perturbing conditions like adding a denaturing agent and applying  
49 thermal stress. The results are further validated by conventional techniques like Dynamic Light Scattering  
50 (DLS) and UV-Vis spectroscopy and Differential Scanning calorimetry (DSC).

51 We report here the results of two studies. First, the interaction of insulin and ZnO, the choice of the system is  
52 based on the demonstrated compatibility of ZnO with insulin<sup>4</sup>. Second, to understand the conformational  
53 changes using protein cleaving enzyme papain. Papain is a heat-resistant enzyme that cleaves peptide bonds of  
54 amino acids including leucine, glycine and cysteine<sup>16, 17</sup>. Since, insulin contains a good amount of these amino  
55 groups, papain severely cleaves it. In our study, the role of papain in denaturing insulin has been observed by  
56 measuring the change in dielectric properties and zeta potential. In addition, we have also studied the thermal  
57 variation of electrical properties of protein complex. Results from these studies demonstrate the effect of  
58 morphologically different MNPs on preserving the electrical configuration of proteins.

## 59 **RESULTS:**

60 **Dielectric Constant of Insulin and Papain.** Thermal variations directly affect the viscosity, intra-molecular  
61 interaction, conformational state variations, and the stability of dimers in proteins<sup>18-20</sup>. We analyzed the thermal  
62 effects on the dielectric constant of insulin and papain in the temperature range between 30 °C and 55 °C at  
63 intervals of 5 °C. For insulin, the dielectric constant was 68 at 30 °C and an increase in temperature was directly  
64 proportional to an increase in dielectric constant, with a maximum of 370 at 55 °C (Fig.1). For papain (high  
65 concentration i.e., 10 mg/ml) at 30 °C, the dielectric constant was 27 which increased to 31 on heating to 55 °C,  
66 and the values for intermediate temperature are shown in Fig.1. Diluted samples of papain (see methods)  
67 showed that the dielectric constant was directly proportional to the papain concentration, as the dielectric  
68 constants were observed to be 24 (30 °C) and 22 (30 °C) for the dilution factors ½ and ¼ respectively. However,  
69 on heating the diluted samples of papain a similar increasing trend in dielectric values was observed, the results  
70 of which are shown in Fig.1. The trend of increasing dielectric constant with temperature agrees with literature  
71 reported on polymers (including papain)<sup>21</sup>. It is evident from the observations and subsequent repeat experiment  
72 that insulin is more sensitive to thermal variation as compared to papain, as reflected in the dielectric constant  
73 variations. In the present work, we have performed two runs to ensure the repeatability of the dielectric  
74 measurements. The average of which has been plotted in Fig.1. It can be seen from the figure that the pure

75 samples show the same values on both runs at the initial temperature. However, the dynamic nature of the  
76 insulin at intermediate temperature adds to the variation in dielectric values. This can be related to the  
77 monomer-dimer equilibrium in insulin which is sustained at room temperature and dissociates on high  
78 temperature ( $>45\text{ }^{\circ}\text{C}$ )<sup>18-20</sup>.

79 **ZnO with insulin and papain.** To test the physicochemical preserving nature of ZnO on insulin and papain,  
80 and the effect of particle morphology on this preserving property, two morphologically different ZnO particles,  
81 Tetrapodal micro particles (ZnO(T) of size  $\sim 15\text{ }\mu\text{m}$ )<sup>22</sup> and ii) Spherical nanoparticles (ZnO(S) of size  $\sim 100\text{ nm}$ )  
82 were used. Besides surface morphology, ZnO(T) is highly crystalline in nature as compared to ZnO(S). Here we  
83 analyzed the effect of ZnO particles on the dielectric constant of insulin and papain, at different temperatures.  
84 When ZnO(S) particles were mixed with insulin, the dielectric constant of the complex (Insulin+ZnO(S)) was  
85  $40\pm 2$  ( $30\text{ }^{\circ}\text{C}$ ) and upon heating, the values increased to  $167\pm 38$  ( $55\text{ }^{\circ}\text{C}$ ). In this case, the rate of increase was not  
86 as significant as it was for pure insulin (i.e., 68 at  $30\text{ }^{\circ}\text{C}$  and 369 at  $55\text{ }^{\circ}\text{C}$ ). When ZnO(T) was mixed in insulin,  
87 the dielectric constant was found to be  $95\pm 14$  ( $30\text{ }^{\circ}\text{C}$ ) which, upon heating increased to  $351\pm 25$  ( $55\text{ }^{\circ}\text{C}$ ).  
88 Interestingly, the complex of Insulin+ZnO(T) exhibited similar dielectric behaviour as that of pure insulin. All  
89 the dielectric constant values for the Fig1 are given in the supplementary file 3.

90 On mixing ZnO particles in papain, it was observed that the dielectric constant of the complex (Papain+ZnO)  
91 increased for all dilutions of papain samples (see Fig.1). This increment was more for samples with ZnO(S) as  
92 compared to samples with ZnO(T). Like all other samples, in this case also, the increase in dielectric constant  
93 was directly proportional to the increase in temperature. As discussed above papain being thermally resistive  
94 shows less increment in its dielectric constant on heating (as compared to insulin), the complex of ZnO and  
95 papain also showed a similar pattern (see Fig. 1). Above results show that the two proteins insulin and papain  
96 having different properties (See table 5 of supplementary file 1) and thus demonstrating different interaction  
97 with MNPs.

98  
99 **Mixing papain and insulin.** Papain denatures other proteins and therefore falls under the category of protease<sup>16</sup>.  
100 In our earlier work, we reported the denaturing effect of papain on egg proteins, plant protein, and insulin. We  
101 found that the dielectric constant decreases on adding papain to proteins<sup>23</sup>. Here, we have extended our  
102 investigation to understand the effect of temperature variation in samples of insulin mixed with different  
103 concentrations of papain. It was observed that on mixing papain with insulin, the net dielectric constant of the  
104 complex decreased significantly. This reduction was proportional to the amount of papain added. Further, on  
105 increasing the temperature for samples mixed with a higher concentration of papain, the dielectric constant  
106 linearly increased and reached a maximum value of 40 at ( $45\text{ }^{\circ}\text{C}$ ) and then eventually decreased on further  
107 heating, this effect was confirmed by performing a control measurement. In the second experiment the maxima  
108 was observed at  $50\text{ }^{\circ}\text{C}$  and then the dielectric values decreased. This variation was absent in samples mixed with  
109 a lower concentration of papain. In fact, for a lower concentration of papain, the dielectric variations on heating  
110 were not significantly different from pure insulin.

111  
112 **Mixing ZnO, with insulin and papain.** After performing the baseline analysis for assessing the effect of  
113 temperature and presence of ZnO and papain on insulin, we further extended the analysis to study the thermal  
114 variations of the denatured complex of insulin and papain and to study the effect of ZnO particles on the same.

115 Having observed that the addition of papain and ZnO decreases and increases the dielectric values of insulin  
116 respectively, we investigated the combined effects of papain and ZnO on insulin. In the mixture containing  
117 insulin, papain and ZnO(T), papain had a denaturing effect on insulin, ZnO(T) exhibited a monotonic increase in  
118 the dielectric values of the denatured insulin with temperature. The dielectric constant for high temperatures was  
119 higher compared to the samples of papain + insulin without ZnO, demonstrating the effect of ZnO(T) on the  
120 thermal behavior of the protein complex. Doing the same analysis on samples of insulin+papain mixed with  
121 ZnO(S), a monotonic increase of the dielectric values (94 to 291±85 for higher, 77±16 to 325 for intermediate  
122 and 36 to 178±27 for lower concentrations, in the temperature range from 30 °C to 55 °C, respectively) was  
123 observed. This change is significantly lesser in comparison to ZnO(T) mixed with insulin+papain (49±12 to  
124 475±97, 49±12.1 to 377 and 25±3 to 130±20 for higher, intermediate and lower concentration respectively in  
125 the temperature range 30 °C to 55 °C). We can observe from the figure that the pure samples show almost  
126 negligible variation on performing repeat dielectric measurements as compared to mixed samples. It is also to be  
127 reported that, when papain was mixed with MNPs, the dielectric variation at high temperature was less as  
128 compared to the samples in which papain was mixed with insulin, suggesting the proteolytic action of papain on  
129 insulin<sup>16,17</sup>.

130 **Thermal effects on mechanical vibration of proteins as pure solutions.** The calculated frequencies of  
131 mechanical vibration through the theoretical model based on dielectric constant, and dipole moment (see  
132 Methods) indicate that the order of mechanical vibrations was  $10^3$  times less than the applied field (of the  
133 resonant antennae used as a probe). Since the resonant frequency of antenna was  $\sim 6.4 \times 10^9$  Hz, the calculated  
134 mechanical vibrations of protein samples were in the MHz range, which corresponds to time interval in the  $\sim \mu\text{s}$   
135 range. The order of time matches well with the findings of Ugo Mayor et. al, in which the group reported that  
136 the collapse of protein into an intermediate native  $\alpha$ -helical secondary structure (a major constituent of  
137 denatured state) happens in time scale of microseconds<sup>24</sup>.

138 On increasing the temperature, the mechanical frequency of insulin decreased, this can be viewed as an effect  
139 resulting from an increased surface area when a protein unfolds. Since the frequency of vibrations (from the  
140 theory of oscillators) depends on mass and length, F.S. Legge et al. performed molecular dynamics (MD)  
141 simulations to see the effect of temperature on the unfolding of insulin, by analyzing the unfolding through  
142 increase in distance between two residues (residue 5 and residue 13) of insulin<sup>25</sup>. Papain being thermally  
143 resistive showed very nominal variation in mechanical frequency on heating. However, we observed that the  
144 mechanical frequencies were significantly different for different concentrations (Fig.2).

145 **Thermal effects on mechanical vibration of proteins in presence of ZnO.** The mechanical frequency of  
146 papain + ZnO(T) and papain + ZnO(S) was less as compared to the relevant same concentration of the pure  
147 solution of papain. The thermal inactivity of papain was observed, as the mechanical frequency did not change  
148 much on increasing the temperature as shown in Fig.2. In contrast, for samples of insulin+ ZnO(S), the  
149 mechanical frequencies (for all temperatures) increased as compared to pure insulin, whereas, for insulin +  
150 ZnO(T) the observed mechanical frequencies were lesser than the frequencies observed for pure insulin. Other  
151 than pure samples and samples mixed with ZnO, the mechanical frequencies were also computed for the  
152 combination of all complexes as it was done for the case of dielectric constant. Significantly, when insulin was  
153 mixed with the higher concentration of papain, the mechanical frequency was nearly constant till 45 °C and

154 then, a sharp increase was observed on further heating to 50 °C. This instant increase in the mechanical  
155 frequency indicates a loss in the mass of protein or fragmentation of protein complex (reduced length).  
156 However, in the presence of ZnO, increment in temperature caused a monotonic reduction in the mechanical  
157 frequency with no anomalies observed at higher temperatures, suggesting the increase in the mass/length of the  
158 MNPs-protein complex.

159 **Verification of theoretically calculated mechanical frequencies.** To verify the theoretically predicted values  
160 of mechanical frequencies which were observed in the MHz range, frequencies of all samples in the close  
161 neighbourhood of theoretical values were pumped into the samples using vector signal generator, with the  
162 pumped power kept fixed at -50 dBm which corresponds to 10  $\mu$ Watts. If the input frequencies match with the  
163 natural frequency of the sample, power is absorbed due to resonant interaction. Using this fact, we found that for  
164 insulin the frequency was 3.5 MHz (45 °C) which is approximately close to the above-predicted value of  
165  $3.237 \pm 0.304$  MHz. Similarly, for other samples also, the observed frequencies were close to the calculated  
166 values with a deviation of no more than 1 MHz in any case. On performing the second run, we found that the  
167 frequencies at which power absorption was noticed remained the same, though, the magnitude of absorption was  
168 different. Mean power absorbed and the standard deviation for all samples are shown in Fig.2.

169 **Validation of results using conventional UV-Vis spectroscopy.** UV-Vis absorption spectroscopy is widely  
170 used to analyze the interaction between proteins and nanoparticles and also to study the conformational changes  
171 (like the formation of the nanoparticles-protein corona)<sup>26, 27</sup>. Events like the unfolding of proteins, mutual  
172 interaction between a diverse variety of proteins, and their binding with nanoparticles can be interpreted based  
173 on careful analysis of the absorbance curve<sup>27</sup>. The wavelength corresponding to the peak absorbance at varying  
174 temperature (20 °C, 30 °C, 40 °C and 50 °C) was measured for all samples, (Table-1). Peak absorbance  
175 wavelength for insulin and papain, as well as for ZnO(T) and ZnO(S) were all found to be close to 282 nm  
176 which did not change much on heating the samples<sup>28-31</sup>. A perceivable redshift (i.e. peak absorbance shift  
177 towards higher wavelength) of 5.0 nm and 3.0 nm was observed on mixing ZnO(S) and ZnO(T) in insulin  
178 respectively. Whereas for papain + ZnO this shift was reduced to 2.0 nm and 1.0 nm for ZnO(S) and ZnO(T)  
179 respectively. A redshift suggests enhanced adsorption of proteins on the surface of the particle<sup>31</sup>. Absorbance  
180 peak at 379 nm and 377 nm were found for ZnO(T) and ZnO(S) respectively but no significant change with  
181 temperature was observed.

182 **Measurement of electrokinetic potential and analyzing surface charge.** The conformational changes in  
183 protein complexes are known to further affect the surface charge properties like the electrokinetic potential of  
184 the slipping plane<sup>32</sup>. Zeta potential is the key parameter to scale the electrostatic interaction in a colloidal  
185 dispersion and is a measure of the electrical stability of the colloid<sup>32</sup>. For pure insulin the Zeta potential was -  
186 12.3 mV which was close to -15 mV as reported<sup>33</sup>, whereas, for papain the Zeta potential was only 6.09 mV  
187 (See Table-2). A positive zeta potential generally evinces the presence of more positive charges in contrast to  
188 the negative charges. Papain enzyme is composed of 24 positively charge amino groups, outnumbering  
189 negatively charged amino groups which are 15, and the zeta potential values reflect the same<sup>34</sup>. On studying the  
190 Zeta potential of insulin + ZnO we found an increase in Zeta potential. For the complex of insulin and tetrapodal  
191 particles, the Zeta potential was -16.7 mV and for the complex of insulin and spherical particles, Zeta potential  
192 was -18.13 mV. These observations correlate with the dielectric variations studied earlier in this manuscript,

193 where we found that the relative change (with respect to pure insulin) in the dielectric constant of  
194 insulin+ZnO(T) was small as compared to insulin + ZnO(S). Zeta potential values of papain+ZnO also show  
195 that spherical ZnO causes a substantial change in the Zeta value (15.2). However, the Zeta Potential of  
196 papain+ZnO(T) showed only a slight increase to 6.68 mV from 6.09 mV (pure papain).

197 **Study of thermodynamic parameters of proteins under thermal transition using DSC.** Results were further  
198 validated using an analytical technique through thermodynamic investigation that directly calculates the change  
199 in enthalpy ( $\Delta H$ ) and specific heat ( $\Delta C_p$ ) of a thermal transition. This change in enthalpy correlates to the  
200 denaturation in terms of heat required for unfolding of a protein<sup>35</sup>. For endothermic process,  $\Delta H$  is a positive  
201 value and for exothermic,  $\Delta H$  is negative. Denaturation involves the uptake of heat required in endothermic  
202 reaction<sup>35</sup>. The positive endothermic DSC peak was found in case of protein and their mixtures with MNPs.  
203 Further, thermograph analysis was performed based on the transition peaks. Also,  $\Delta H$  and the temperature  
204 corresponding to peak value in the thermograph ( $T_m$ ) for heat denaturation were  $69.67 \pm 10.63$  (J/g °C),  
205  $(52.78 \pm 1.49)$  °C for insulin and  $103.28 \pm 22.73$  (J/g °C), and  $(59.43 \pm 4.16)$  °C for papain respectively.  $\Delta H$  value  
206 for insulin mixed with MNPs was closer to the insulin as compared to the insulin mixed with papain (See Table-  
207 3). Maximum enthalpy change is found for Insulin+papain which validate the volatile behavior of papain as  
208 observed in dielectric studies.

#### 209 **Discussion:**

210 The above stated results indicate variation in dielectric constant due to atomic and molecular interaction owing  
211 to temperature dependent protein unfolding or denaturation. The dipole fluctuation depends on both collective  
212 large-scale motions<sup>15</sup> and local motions<sup>15</sup>, therefore, probing the dipole fluctuation or the dipole moment through  
213 measurement of dielectric constant can offer deeper understanding on the interaction mechanism of MNPs and  
214 proteins and their unfolding. In the type of system which we dealt with, it can be assumed that the MNP-protein  
215 complex is acted upon by binding force due to chemical bonding, driving force due to applied field and the  
216 damping force offered by the buffer in which MNP-protein complex was dispersed. The mechanical frequency  
217 of the protein complex was calculated using the proposed theoretical model based on the dielectric constant and  
218 dipole moment (See Methods Section). This parameter aided in understanding the interaction taking place at the  
219 molecular level. Fig 3 illustrates the interaction of insulin with MNPs and papain. Physical properties such as  
220 dielectric constant, dipole moment, polarization current density and zeta potential of Insulin+ZnO(T) (IZnO(T))  
221 are closer to insulin as compared to Insulin+ZnO(S) (IZnO(S)), Insulin+ZnO(S)+Papain (IZnO(S)P) and  
222 Insulin+ZnO(T)+Papain (IZnO(T)P). This study concludes that shape and surface morphology of MNPs can  
223 affect or preserve the electrical configuration of protein. The ZnO(T) structures can preserve the polarity and  
224 spatial-surface charge distribution of protein, therefore, can be effective carriers and preservatives for insulin.  
225 Overall, this study offers novelty in understanding bio-molecular interaction, the variation in electrical  
226 properties of protein during MNPs interaction indicating sensitivity to atomic and molecular interaction  
227 changes. Thus, exploring the electrical properties of the MNP-Protein complex and their optimal variation  
228 compared with the corresponding pure protein sample can provide a better understanding of the functionality,  
229 stability, and interaction, etc. Dielectric results were further validated using DSC, the enthalpy measurements  
230 from DSC agree with the dielectric results. This has implications for nano-drug design, where nanoparticles tend  
231 to change the surface electrical properties of MNP-Protein corona and thereby change the functional properties

232 of proteins. Such studies have the potential to overcome or address the slow or not very successful translation of  
 233 nano-medicine<sup>36-40</sup>.

234

## 235 **Material and Methods**

236 **Materials:** Insulin Humalog (Powder type) purchased from Sigma Aldrich was diluted in HEPES Buffer (50.7  
 237 ml of distilled water, 1.3 ml of HEPES Buffer) at a final concentration of 6.9 mg/ml. For understanding the NP-  
 238 Protein interaction, ZnO(S) and ZnO(T) were used. ZnO(S) (<100 nm) is purchased from Sigma Aldrich  
 239 whereas ZnO(T) are synthesised using flame transport synthesis method by Functional Nano-material group, Kiel  
 240 University, Germany<sup>41</sup>. The NPs are prepared in distilled water at a final concentration 3.45 mg/ml. Further  
 241 studying denaturation, the strong protease enzyme (Papain) purchased from BIOENZYME and prepared in  
 242 distilled water and cleaned through vacuum pump. Three different dilutions (1/2<sup>n</sup>) of the papain P1 (10 mg/ml),  
 243 P2 (5 mg/ml) and P3 (2.5 mg/ml) have been selected for dielectric measurements. All solutions were prepared  
 244 freshly when used for measurements. All the sample concentration discussed above is used for dielectric  
 245 measurement. However, Electrophoretic and UV-VIS spectroscopy cannot work with high concentration  
 246 because of creating turbulence. Thus 100 µl of each solution (ZnO(S), ZnO(T), P1 and insulin) mixed with 900  
 247 µL of distilled water (for ZnO(S), ZnO(T) and P1) and HEPES buffer (for Insulin). For all techniques, the  
 248 mixing ratio was fixed i.e., 2:1 for Insulin and NPs, 10:1 for insulin and papain, 8:1:4 for insulin, papain and  
 249 NPs. Detailed protocol of sample preparation and mixing ratio is discussed in supplementary file (See  
 250 [supplementary file 1](#)).

251 **Methods:** The dielectric measurements performed with the coaxial fork type probe designed at 6.45 GHz. The  
 252 near field region of probe is less than 10 cm thus does not sense the noise of surrounding. Technique is reliable  
 253 in terms of giving quick and repeatable results. This technique is based on the shift in the resonating frequency  
 254 due to placing sample in front of the probe. For the present studies, we put the sample solution into  
 255 polypropylene made sample holder (250 µL Holding capacity) then heat it using hotplate for the range 30 °C to  
 256 55 °C. To make heating effectively, the isolated box was used for thermal insulation and experimental setup is  
 257 discussed in supplementary file (See [supplementary file 2](#)). The method of calculating the dielectric constant is  
 258 also previously reported<sup>23</sup>.

259 **Mechanical Frequency, Dipole moment and Polarization current density measurements:** To further  
 260 understand phenomenon taking place at molecular level, a theoretical model was developed where it is assumed  
 261 that the NP protein complex suspended in a buffer medium is governed by three forces (binding, damping and  
 262 driving forces) and solving for the governing differential equations (See [supplementary file 2](#)) a theoretical  
 263 expression for mechanical vibration frequency, dipole moment and polarization current density were derived  
 264 which are dielectric constant dependent (See [supplementary file 2](#)).

$$\epsilon_r = 1 + \frac{NQ^2(\omega_0^2 - \omega^2)}{M\epsilon_0[(\omega_0^2 - \omega^2)^2 + (\gamma\omega)^2]} \quad (1)$$

265

$$\omega_0^2 = \frac{\left[ \frac{NQ^2}{M\epsilon_0(\epsilon_r-1)} + 2\omega^2 \right] \pm \sqrt{\left[ \frac{NQ^2}{M\epsilon_0(\epsilon_r-1)} + 2\omega^2 \right]^2 - 4 \left( \frac{NQ^2}{M\epsilon_0(\epsilon_r-1)} + 2\omega^2 \right) \left( \omega^4 + \gamma^2\omega^2 + \frac{NQ^2\omega^2}{M\epsilon_0(\epsilon_r-1)} \right)}}{2} \quad (2)$$

266

$$\tilde{P}(t) = \left[ \frac{NQ^2(\omega_0^2 - \omega^2)E_0}{M\epsilon_0[(\omega_0^2 - \omega^2)^2 + (\gamma\omega)^2]} + i \frac{\gamma\omega NQ^2E_0}{M\epsilon_0[(\omega_0^2 - \omega^2)^2 + (\gamma\omega)^2]} \right] e^{-i\omega t} \quad (3)$$

267

$$J_P = \frac{NQ^2(\omega_0^2 - \omega^2)E_0}{M[(\omega_0^2 - \omega^2)^2 + (\gamma\omega)^2]} (\gamma\omega^2 \cos(\omega t) - (\omega_0^2 - \omega^2)\omega \sin(\omega t)) \quad (4)$$

268

269 Where N, M and Q are number of molecules, mass of molecule and charge on molecule whereas  $\omega$ ,  $\epsilon_r$  and  $E_0$  is  
 270 frequency of driven electric field, dielectric constant, amplitude of electric field. The mechanical frequency ( $\omega_0$ ),  
 271 dipole moment (P) and polarization current density ( $J_P$ ) of any polar molecule can be calculated by knowing the  
 272 N, Q, M,  $\omega$ ,  $\epsilon_r$ ,  $E_0$  and  $\gamma$ . Where  $\gamma$  is known as damping constant and in the present method it is assumed  
 273 empirical parameter and estimated by the known dipole moment. The dipole moment of insulin and papain are  
 274 369 and 150 Debye as reported in literature<sup>42-44</sup>. And for mixing case,  $\gamma$  is calculated using the following  
 275 equation.

$$\gamma_{mixed} = \gamma_1 \frac{V_1}{V_{Total}} + \gamma_2 \frac{V_2}{V_{Total}} \quad (5)$$

276

277 And the factor  $\frac{NQ^2}{M}$  is calculated for the mixing case using the following equation

$$\frac{NQ^2}{M} = \frac{N_1 Q_1^2}{M_1} + \frac{N_2 Q_2^2}{M_2} \quad (6)$$

278

279 The parameters Q and M are perceived through literature<sup>42-46</sup>. For insulin Q and M are  $74.805 \times 10^{-10}$  coulomb  
 280 and  $9.52 \times 10^{-18}$  Kg respectively whereas for papain  $4.01 \times 10^{-8}$  coulomb and  $3.88 \times 10^{-17}$  kg respectively. The  
 281 value of N is estimated through concentration and volume of the sample and also size and mass of the molecule.  
 282 ZnO, with its almost 0 net-charge and significantly higher mass compared to insulin and papain, is neglected.  
 283 The electric field is 4.9 V/m which is calculated using the power delivered by the antenna and the distance  
 284 between ground plane and tip of the probe. Here the driving frequency is the resonating frequency of probe  
 285 antenna i.e., 6.41GHz. Here in equation, the time t is taken 1 microsecond close to protein relaxation time<sup>47</sup>.

## 286 **References:**

287 [1] Klein, J. Probing the interactions of proteins and nanoparticles. *Proceedings of the National Academy of*  
 288 *Sciences***104**, 2029–2030 (2007).

289 [2] Cedervall, T. *et al.* Understanding the nanoparticle–protein corona using methods to quantify exchange rates  
 290 and affinities of proteins for nanoparticles. *Proceedings of the National Academy of Sciences***104**, 2050–2055  
 291 (2007).

- 292 [3] Cedervall, T. *et al.* Detailed identification of plasma proteins adsorbed on copolymer nanoparticles.  
293 *Angewandte Chemie International Edition* **46**, 5754–5756 (2007).
- 294 [4] Jiang, J., Pi, J. & Cai, J. The advancing of zinc oxide nanoparticles for biomedical applications. *Bioinorganic*  
295 *chemistry and applications*, (2018).
- 296 [5] Word, J. M., Lovell, S. C., Richardson, J. S. & Richardson, D. C. Asparagine and glutamine: using hydrogen  
297 atom contacts in the choice of side-chain amide orientation. *Journal of molecular biology* **285**, 1735–1747  
298 (1999).
- 299 [6] Kumar, S. & Nussinov, R. How do thermophilic proteins deal with heat? *Cellular and Molecular Life*  
300 *Sciences CMLS* **58**, 1216–1233 (2001).
- 301 [7] Matthew, J. B. Electrostatic effects in proteins. *Annual review of biophysics and biophysical chemistry* **14**,  
302 387–417 (1985).
- 303 [8] Bibi, F., Villain, M., Guillaume, C., Sorli, B. & Gontard, N. A review: Origins of the dielectric properties of  
304 proteins and potential development as bio-sensors. *Sensors* **16**, 1232 (2016).
- 305 [9] Richards, E. G. & Dover, S. D. *An introduction to the physical properties of large molecules in solution*. vol.  
306 3 (CUP Archive, 1980).
- 307 [10] Basey-Fisher, T. *et al.* Microwave Debye relaxation analysis of dissolved proteins: Towards free-solution  
308 biosensing. *Applied Physics Letters* **99**, 233703 (2011).
- 309 [11] Wolf, M., Gulich, R., Lunkenheimer, P. & Loidl, A. Relaxation dynamics of a protein solution investigated  
310 by dielectric spectroscopy. *Biochimica et Biophysica Acta (BBA)-Proteins and Proteomics* **1824**, 723–730  
311 (2012).
- 312 [12] Nakanishi, M. & Sokolov, A. P. Protein dynamics in a broad frequency range: Dielectric spectroscopy  
313 studies. *Journal of Non-Crystalline Solids* **407**, 478–485 (2015).
- 314 [13] Li, L., Li, C., Zhang, Z. & Alexov, E. On the dielectric “constant” of proteins: smooth dielectric function for  
315 macromolecular modeling and its implementation in DelPhi. *Journal of chemical theory and computation* **9**,  
316 2126–2136 (2013).
- 317 [14] Simonson, T. & Brooks, C. L. Charge screening and the dielectric constant of proteins: insights from  
318 molecular dynamics. *Journal of the American Chemical Society* **118**, 8452–8458 (1996).
- 319 [15] Bourgeat, L., Serghei, A. & Lesieur, C. experimental protein Molecular Dynamics: Broadband Dielectric  
320 Spectroscopy coupled with nanoconfinement. *Scientific reports* **9**, 1–12 (2019).
- 321 [16] <https://www.sigmaaldrich.com/life-science/metabolomics/enzyme-explorer/analytical-enzymes/papain.html>
- 322 [17] Babu, K. M. 5 - The dyeing of silk. in *Silk (Second Edition)* (ed. Babu, K. M.) 109–128 (Woodhead  
323 Publishing, 2019). doi:10.1016/B978-0-08-102540-6.00005-X.
- 324 [18] Chauhan, B. *Principles of biochemistry and biophysics*. (Firewall Media, 2008).

- 325 [19] Abramson, H., Gorin, M. & Moyer, L. The Polar Groups of Protein and Amino Acid Surfaces in Liquids.  
326 *Chemical Reviews***24**, 345–366 (1939).
- 327 [20] Bekard, I. B. & Dunstan, D. E. Tyrosine autofluorescence as a measure of bovine insulin fibrillation.  
328 *Biophysical journal***97**, 2521–2531 (2009).
- 329 [21] Muthulakshmi, S., Iyyapushpam, S. & D PATHINETTAM, P. Effect of temperature on the AC impedance  
330 of protein and carbohydrate biopolymers. *Bulletin of Materials Science***37**, 1575–1582 (2014).
- 331 [22] Mishra, Y. K. & Adelung, R. ZnO tetrapod materials for functional applications. *Materials Today***21**, 631–  
332 651 (2018).
- 333 [23] Urvashi et. al. Measurement of Dielectric Properties of Biological Materials Using Co-Axial Fork-Type  
334 Probe. *IEEE Sensors Journal***19**, 10482–10489 (2019).
- 335 [24] Mayor, U. *et al.* The complete folding pathway of a protein from nanoseconds to microseconds. *Nature***421**,  
336 863–867 (2003).
- 337 [25] Legge, F., Budi, A., Treutlein, H. & Yarovsky, I. Protein flexibility: multiple molecular dynamics  
338 simulations of insulin chain B. *Biophysical chemistry***119**, 146–157 (2006).
- 339 [26] Kharazian, B., Hadipour, N. & Ejtehadi, M. Understanding the nanoparticle–protein corona complexes  
340 using computational and experimental methods. *The international journal of biochemistry & cell biology***75**,  
341 162–174 (2016).
- 342 [27] Poklar, N. & Vesnaver, G. Thermal denaturation of proteins studied by UV spectroscopy. *Journal of*  
343 *Chemical Education***77**, 380 (2000).
- 344 [28] Bai, Z. *et al.* Partitioning behavior of papain in ionic liquids-based aqueous two-phase systems. *Journal of*  
345 *Chemistry***2013**, (2013).
- 346 [29] Vanaja, A., Suresh, M. & Jeevanandam, J. Facile Magnesium Doped Zinc Oxide Nanoparticle Fabrication  
347 and Characterization for Biological Benefits. *International Journal of Nanoscience and Nanotechnology***15**,  
348 277–286 (2019).
- 349 [30] Correia, M., Neves-Petersen, M. T., Jeppesen, P. B., Gregersen, S. & Petersen, S. B. UV-light exposure of  
350 insulin: pharmaceutical implications upon covalent insulin dityrosine dimerization and disulphide bond  
351 photolysis. *PloS one***7**, e50733 (2012).
- 352 [31] Casals, E., Pfaller, T., Duschl, A., Oostingh, G. J. & Puentes, V. Time evolution of the nanoparticle protein  
353 corona. *ACS nano***4**, 3623–3632 (2010).
- 354 [32] Bhattacharjee, S. DLS and zeta potential—what they are and what they are not? *Journal of controlled*  
355 *release***235**, 337–351 (2016).
- 356 [33] Taluja, A. & Bae, Y. H. Role of a novel excipient poly (ethylene glycol)-b-poly (L-histidine) in retention of  
357 physical stability of insulin at aqueous/organic interface. *Molecular pharmaceutics***4**, 561–570 (2007).

- 358 [34] Tigist, M. *et al.* Extraction and purification of papain enzyme from papaya leaf and the phytochemical  
359 components of the leaf. (2016).
- 360 [35] Ansari MJ *et. al.* Enhanced oral bioavailability of insulin-loaded solid lipid nanoparticles: pharmacokinetic  
361 bioavailability of insulin-loaded solid lipid nanoparticles in diabetic rats. *Drug delivery*. Jul 23;23(6):1972-9  
362 (2016)
- 363 [36] Dyawanapelly, S. *et al.* How the surface functionalized nanoparticles affect conformation and activity of  
364 proteins: Exploring through protein-nanoparticle interactions. *Bioorganic chemistry* **82**, 17–25 (2019).
- 365 [37] Chen, X. *et al.* Conformational manipulation of scale-up prepared single-chain polymeric nanogels for  
366 multiscale regulation of cells. *Nature Communications* **10**, 2705 (2019).
- 367 [38] Brouwer, P.J.M., Antanasijevic, A., Berndsen, Z. *et al.* Enhancing and shaping the immunogenicity of  
368 native-like HIV-1 envelope trimers with a two-component protein nanoparticle. *Nat Commun* **10**, 4272 (2019).
- 369 [39] Lu, X., Xu, P., Ding, HM. *et al.* Tailoring the component of protein corona via simple chemistry. *Nat*  
370 *Commun* **10**, 4520 (2019).
- 371 [40] Mahmoudi, M., Bertrand, N., Zope, H. & Farokhzad, O. C. Emerging understanding of the protein corona at  
372 the nano-bio interfaces. *Nano Today* **11**, 817–832 (2016).
- 373 [41] Y. K. Mishra *et. al.* *Part. Part. Syst. Charact.*, **30**, 775 (2013)
- 374 [42] Takashima, S. & Asami, K. Calculation and measurement of the dipole moment of small proteins: use of  
375 protein data base. *Biopolymers: Original Research on Biomolecules* **33**, 59–68 (1993).
- 376 [43] VanDuijnen, P. T., Thole, B. T. & Hol, W. On the role of the active site helix in papain, an ab initio  
377 molecular orbital study. *Biophysical chemistry* **9**, 273–280 (1979).
- 378 [44] Felder, C. E., Prilusky, J., Silman, I. & Sussman, J. L. A server and database for dipole moments of  
379 proteins. *Nucleic acids research* **35**, W512–W521 (2007).
- 380 [45] Waugh, D. F. A fibrous modification of insulin. I. The heat precipitate of insulin. *Journal of the American*  
381 *Chemical Society* **68**, 247–250 (1946).
- 382 [46] [https://www.bioinformatics.org/sms/prot\\_mw.html](https://www.bioinformatics.org/sms/prot_mw.html)
- 383 [47] Erickson, H. P. Size and shape of protein molecules at the nanometer level determined by sedimentation,  
384 gel filtration, and electron microscopy. *Biological procedures online* **11**, 32–51 (2009).
- 385

### 386 Acknowledgments

387 We present sincere thanks to Dr. Madhan Tirumalai from University of Houston (Department of Biology and  
388 Biochemistry), for proof reading and suggesting appropriate corrections for the manuscript. We acknowledge  
389 the support from Dr. Prem Saran Tirumalai from the Department of Botany, DEI, for the use of papain in the  
390 present work. We acknowledge the support from Late Prof. Manmohan Srivastava, Prof. Sahab Dass Kaura and  
391 Prof. Soami Pyara and Dr. Sudhir Kumar Verma from the Department of Chemistry, DEI, Agra for providing  
392 access to their Instrument lab for DLS, UV-Vis and DSC studies. This project was funded in parts by University  
393 Grant Commission (UGC) through Capital Asset Grant and in parts by UGC Special Assistance Program.

394

395 **Author contributions**

396 K. S. Daya and Urvashi conceived the idea, Urvashi and K. S. Daya designed the experiment. Urvashi  
 397 performed the experiment and Urvashi, K. S. Daya, Zeeshan, Rainer Adelung, Mridul Kumar, Martina Baum,  
 398 and Armin Reimers carried out data analysis. Urvashi, Zeeshan and K.S. Daya drafted the manuscript and all  
 399 authors contributed to the editing of paper.

400

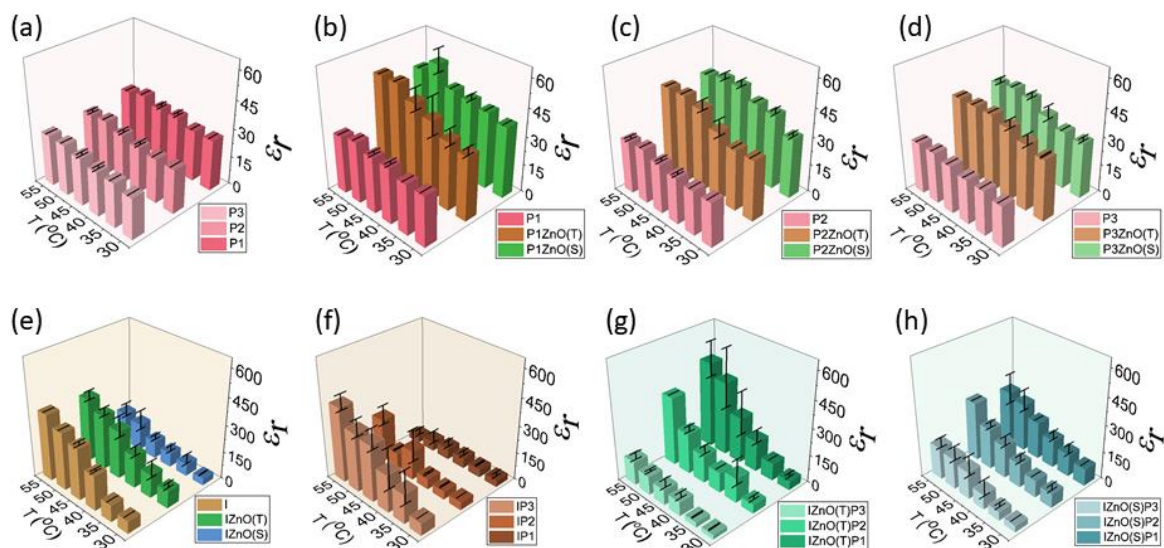
401 **Competing interests**

402 The authors declare no competing interests.

403

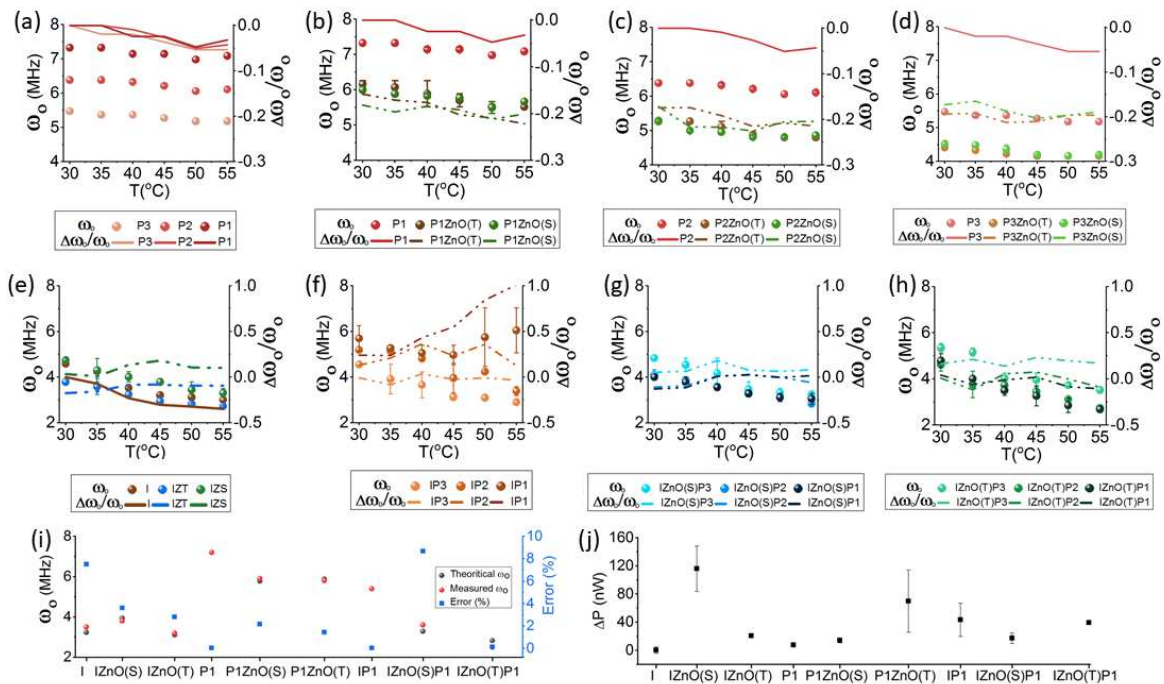
404 **Additional information**

405 Correspondence and requests for materials should be addressed to K. S. Daya (ksdaya@dei.ac.in)



406

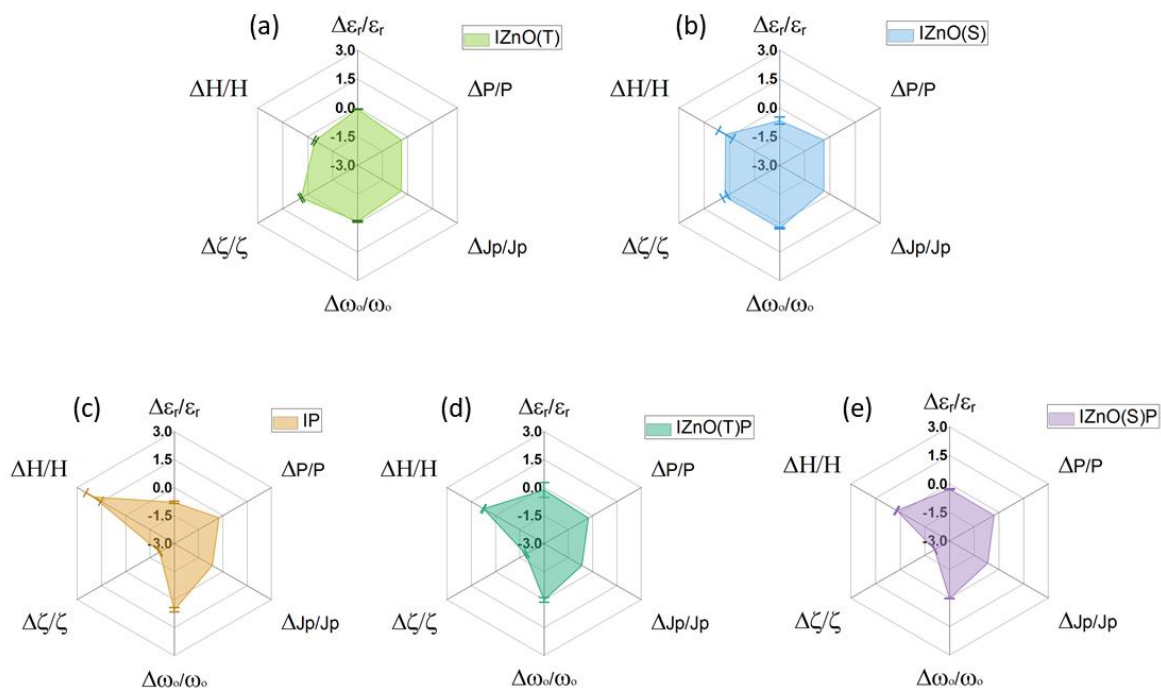
407 Figure 1 Dielectric constant of (a) Papain of three dilutions (b-d) and mixed with ZnO(S) and ZnO(T) (e) Insulin  
 408 and Insulin mixed with ZnO(S) and ZnO(T) (f) Insulin mixed with three different dilutions of papain (g) Insulin  
 409 mixed with ZnO(T) and Papain (h) Insulin mixed with ZnO(S) and Papain. Here the abbreviations P1, P2 and  
 410 P3: Higher, Intermediate and lower concentration of Papain and I: Insulin and  $\epsilon_r$ : dielectric constant.



411

412

413 Figure 2 Theoretically proposed Mechanical Frequency ( $\omega_0$ ) of (a) Papain of three dilutions (b-d) and mixed  
 414 with ZnO(S) and ZnO(T) (e) Insulin and Insulin mixed with ZnO(S) and ZnO(T) (f) Insulin mixed with three  
 415 different dilutions of papain (g) Insulin mixed with ZnO(S) and Papain. (h) Insulin mixed with ZnO(T) and  
 416 Papain (Here the average of theoretical mechanical frequency is plotted. Where the bar shows two runs executed  
 417 as in case of dielectric constant) (i) Measured and Theoretical mechanical frequency using Spectroscopic  
 418 technique and theoretical proposed model respectively and the corresponding relative error with the theoretical  
 419 (Here the value corresponding to 45 °C and the case at 50 °C discussed in supplementary file 2) (j) the Average  
 420 power changed of sample, the Experiment was performed twice. So, the bars indicate the variation of two runs.  
 421 Here P1, P2 and P3: Higher, Intermediate and lower concentration of Papain and I: Insulin.



422

423

424 Figure 3 Radar chart of correlation of physical parameters (The abbreviation  $\epsilon_r$ , P, Jp,  $\omega_o$ ,  $\zeta$  and H are used for  
 425 physical parameters dielectric constant, dipole moment, polarization current density, mechanical frequency zeta  
 426 potential and enthalpy), These Y chart values are relative change (with respect to Insulin) for various samples  
 427 which suggest the deviation from the physical parameter of Insulin. Norman cloture for papain sample P is used  
 428 here because P is carried with different concentration in these techniques. Here for microwave spectroscopy P1  
 429 (Highest concentration) is used and the lower dilutions were used for zeta potential measurement because high  
 430 concentrations are not suitable in these studies due to turbulence. The detail protocol of sample preparation was  
 431 discussed in the supplementary file 1. Although, mixing ratio is same in all.

432

433

434 Table 1 The measured wavelength corresponding to the absorbance peak of all samples at various temperatures  
 435 (20 °C, 30 °C, 40 °C and 50 °C) using UV Spectrophotometer

436

Wavelength (nm)

T(°C)	Pure Samples				Mixed Samples						
	ZnO(S)	ZnO(T)	I	P	IZnO(S)	IZnO(T)	PZnO(S)	PZnO(T)	IP	IZnO(S)P	IZnO(T)P
20	282*	283	285	283	287	286	284	284	285	284	285
30	282	282	284	282	287	284	282	282	284	282	284
40	282	282	284	282	286	287	283	282	284	282	285
50	282	282	284	282	285	285	283	282	284	282	285

Table 2 Measured Zeta potential (DLS data) of the samples

Zeta Potential (mV)

	Pure Samples				Mixed Samples						
	ZnO(S)	ZnO(T)	I	P	IZnO(S)	IZnO(T)	PZnO(S)	PZnO(T)	IP	IZnO(S)P	IZnO(T)P
Run1	-10.9	-19.9	-12.3	5.98	-17.3	-16.2	15.2	6.38	13.5	13.3	9.96
Run2	-10.4	-21.2	-11.7	6.68	-18.3	-16.7	15.2	6.84	12.9	13	11
Run3	-11.4	-16.4	-12.9	5.62	-18.8	-17.4	15.3	6.84	13.4	12.4	11.7
Avg	-10.9	-19.1	-12.3	6.09	-18.1	-16.7	15.2	6.68	13.2	12.9	10.88

Table 3 DSC measurements of samples ( $\Delta H$ : average change in enthalpy,  $T_m$ : average temperature corresponding to peak value in DSC thermograph curve having range 30 °C-100 °C,  $\Delta C_p$ : average change in specific heat,  $T_g$ : average temperature at half  $C_p$  extrapolated,  $\delta$ : variation of two independent runs. Scan rate 20 °C/minute)

S. No	Sample	$(\Delta H \pm \delta)$ J/g °C	$(T_m \pm \delta)$ °C	$(\Delta C_p \pm \delta)$ J/g °C	$(T_g \pm \delta)$ °C
1.	I	69.67±10.63	52.78±1.49	2.10±0.08	37.83±0.40
2.	P	103.28±22.73	59.43±4.16	3.64±0.42	41.14±1.49
3.	ZnO(S)	8.08±1.50	49.82±1.17	0.18±0.02	38.23±5.75
4.	ZnO(T)	7.13±1.07	40.82±4.47	0.53±0.30	33.44±0.47
5.	IZnO(S)	62.15±1.25	46.61±0.01	2.19±0.05	34.60±0.07
6.	IZnO(T)	38.26±1.22	50.46±0.51	2.08±0.61	37.47±1.06
7.	PZnO(S)	107.70±7.01	51.26±0.33	4.24±0.03	37.83±0.27
8.	PZnO(T)	125.35±11.45	53.08±0.18	4.78±0.08	39.19±0.09
9.	IP	213.35±64.19	58.58±0.02	6.38±1.79	43.42±0.86
10.	IZnO(S)P	83.67±10.94	56.13±5.18	3.10±0.11	40.69±2.08
11.	IZnO(T)P	120.44±16.36	53.10±0.16	4.22±0.55	38.64±0.21

## Supplementary Files

This is a list of supplementary files associated with this preprint. Click to download.

- [2.Supplementaryprotocol.docx](#)
- [3.Supplementaryexptsetupmodel.docx](#)
- [4.Supplementarydata.docx](#)